Article

Monitoring and Prediction of Wild Blueberry Phenology Using a Multispectral Sensor

Kenneth Anku [1],* , **David Percival [1], Mathew Vankoughnett [2], Rajasekaran Lada [1] and Brandon Heung [1]**

[1] Department of Plant, Food, and Environmental Sciences, Dalhousie University, 50 Pictou Road, Truro, NS B2N 5E3, Canada; david.percival@dal.ca (D.P.); raj.lada@dal.ca (R.L.); brandon.heung@dal.ca (B.H.)

[2] Center of Geographic Sciences, Nova Scotia Community College, 50 Elliott Road, Halifax, NS B0S 1M0, Canada; mathew.vankoughnett@nscc.ca

* Correspondence: kenneth.anku@dal.ca; Tel.: +1-(902)-706-0034

Abstract: (1) Background: Research and development in remote sensing have been used to determine and monitor crop phenology. This approach assesses the internal and external changes of the plant. Therefore, the objective of this study was to determine the potential of using a multispectral sensor to predict phenology in wild blueberry fields. (2) Method: A UAV equipped with a five-banded multispectral camera was used to collect aerial imagery. Sites consisted of two commercial fields, Lemmon Hill and Kemptown. An RCBD with six replications, four treatments, and a plot size of 6 × 8 m with a 2 m buffer between plots was used. Orthomosaic maps and vegetative indices were generated. (3) Results: There were significant correlations between VIs and growth parameters at different stages. The F4/F5 and F6/F7 stages showed significantly high correlation values among all growth stages. LAI, floral, and vegetative bud stages could be estimated at the tight cluster (F4/F5) and bloom (F6/F7) stages with R^2/CCC = 0.90/0.84. Variable importance showed that NDVI, ENDVI, GLI, VARI, and GRVI contributed significantly to achieving these predicted values, with NDRE showing low effects. (4) Conclusion: This implies that the F4/F5 and F6/F7 stages are good stages for making phenological predictions and estimations about wild blueberry plants.

1. Introduction

The wild blueberry plant, commonly referred to as the "lowbush" blueberry, is a perennial calcifuge shrub managed on large commercial fields. These fields are largely dominated by two species, *Vaccinium angustifolium* and *V. myrtilloides* [1]. Management practices require a two-year production cycle consisting of vegetative and cropping years. Several diseases affect the plant, but the most common in the cropping year are the Monilinia blight (MB) and Botrytis blossom blight (BB) diseases, which affect plant foliage and flowers, respectively [2,3]. However, the plant's disease susceptibility depends on the phenological stage and phenotype.

Monitoring phenology in the field is crucial for managing and producing wild blueberries. The phenological difference in phenotypes, slope direction, and surrounding vegetation creates a varying pattern of disease damage. The *Vaccinium myrtilloides* phenotype observes a delayed growth pattern, reproductive budburst, and flowering late by a week when compared with *V. angustifolium* [4]. The methods for carrying out field

assessments on growth and development stages have always depended on physical monitoring, which adopts a destructive approach. Therefore, to determine growth parameters, plants are destroyed, and this affects the plant population structure. Different methods and approaches have been adopted in monitoring wild blueberry phenology including the use of weather data and monitoring the morphological traits [5]. However, this approach still poses challenges, as these methods are not always accurate, require extensive field scouting by experienced personnel, and are time-consuming and expensive. The advancement in the use of remote sensing (RS) has allowed predictions and determinations to be made using VIs. These VIs are mathematical computations or ratios of the different wavelengths reflected from vegetation [6,7]. Several studies adopting VIs have been utilized to make phenological determinations and predictions on crops including cotton, rice, and wheat [7,8]. Therefore, the physiological changes being observed in the wild blueberry field as a result of upright stem growth and development can be monitored aerially using remote sensing approaches. This allows for early field evaluation and possible predictions or estimations of growth parameters.

The use of remote sensing technologies and machine learning (ML) approaches has become a routine activity for early field-scale evaluations to support management and production practices through the application of computational algorithms such as support vector machines (SVMs) and random forests (RFs) [9,10]. Unmanned aerial vehicles (UAVs) mounted with different sensors have been used to acquire imagery to compute VIs in extracting information from remotely sensed data [7,11]. Thus, VIs have been adapted to monitor phenology and determine other growth parameters such as leaf area, stem branches, nitrogen content, and plant height, among other plant parameters [12]. Recent developments in remote sensing have used VIs such as the normalized difference vegetative index (NDVI) to monitor and estimate phenology [13,14]. Several studies have also demonstrated the possibility of using VIs such as the green leaf index (GLI) and normalized difference red edge index (NDRE) to monitor plant growth and development in many crops, including sunflower [15], rice [16,17], rapeseed [13,14], wheat [7], cotton [8], and wild blueberries [18]. Outcomes from these studies, using their correlation and coefficient of determination values, have demonstrated accuracy in monitoring and estimating growth and development parameters in the field. Despite the progress in some initial works conducted by Maqbool et al. [19], Anku et al. [11,18], Barai et al. [20], and Pare et al. [21] in monitoring growth parameters and improving management practices, these studies used simple techniques that focused on a limited number of VIs, and they were limited to a few growth parameters. In a similar survey conducted, Forsström et al. [12] assessed the seasonal dynamics of lingonberry and blueberry; however, their study focused on highbush blueberry using the hyperspectral technique. A recent study by MacEachern et al. [22] highlighted the potential of monitoring and prediction; however, their study focused only on predicting wild blueberry yield. Although significant progress has been made, remote sensing activities in wild blueberry fields have received little attention for their potential to enhance yield, growth, and development, as well as to reduce the overall cost of management and production practices. However, the adoption of multispectral technology using VIs for the assessment of growth and development coupled with machine learning approaches in wild blueberries is still lacking.

Considering the relevance and utilization of these precision agricultural techniques in crop production, there is the potential to apply these remote sensing approaches in monitoring plant growth and development in wild blueberries. Given this, the study was conducted on the wild blueberry field using a multispectral sensor (i) to determine the potential of using machine learning approaches to predict plant height (PH), floral and

vegetative buds, leaf area index (LAI), and yield and (ii) to determine the best phenological stage where predictions can be made.

2. Materials and Methods

2.1. Study Area

This study was conducted in the 2020 growing season in two locations, namely the Lemmon Hill and Kemptown fields (Figure 1A). These commercial fields are located in Colchester County in Nova Scotia, Canada, with the following geographic coordinates: 45.188587°N, 62.874343°W for Lemmon Hill and 45.498936°N, 63.100716°W for Kemptown. The two trial sites are old commercial wild blueberry fields that have undergone several years of cultivation with adequate plant coverage and minimized occurrence of bare areas or weed patchiness, making them a good representation for this trial. These fields are prone to wet conditions that can be encountered for an extended period, thus the need for disease-controlling fungicides to mitigate the devasting effects of the Monilinia and Botrytis blight diseases on the field, which affect plant yield [23]. These fields have good climatic conditions, with an annual rainfall of between 1550 mm to 2000 mm and a temperature range of between 16 °C to 22 °C in the month of May for agricultural activities. The two fields were at the same cropping phase of production, with substantial variability among vegetation, equal plant coverage, and the same plant stage.
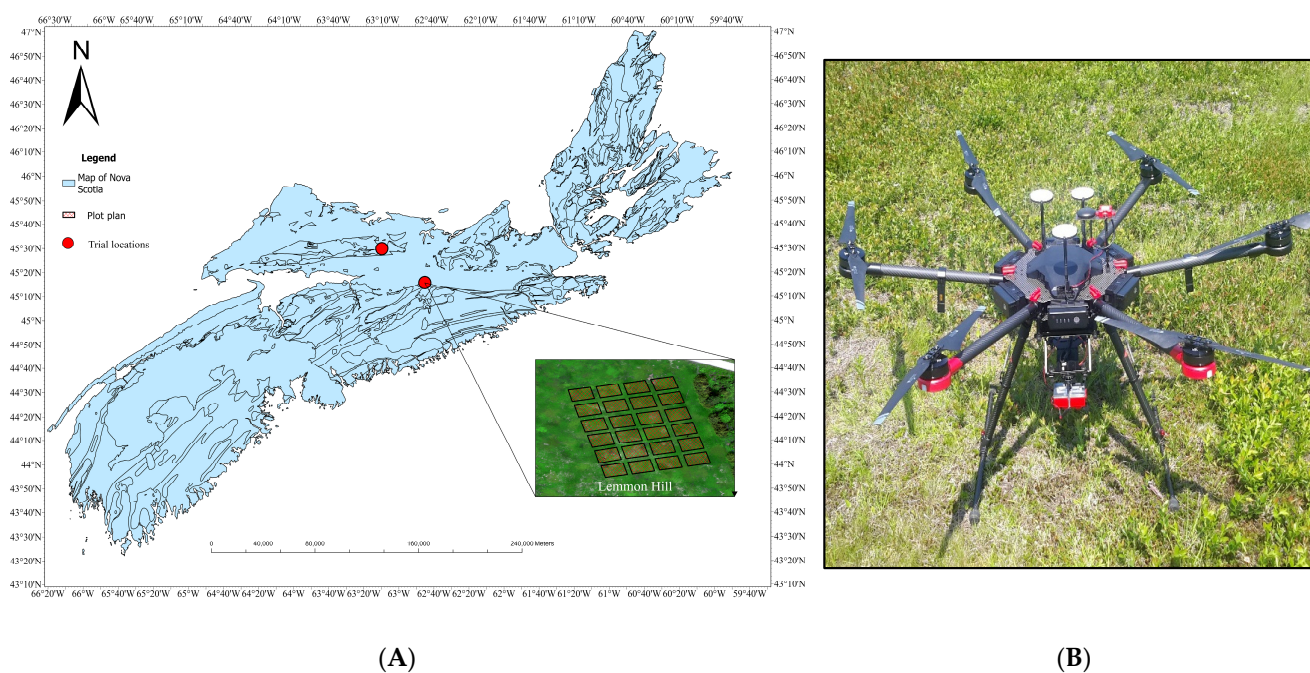

(A)   **(B)**

Figure 1. (**A**) Lemmon Hill trial site showing individual plots at the study area, and (**B**) the DJI Matrice 600 Pro UAV equipped with a 5-banded MicaSense camera.

2.2. Experimental Design

The experimental design for these trials was a randomized complete block design with six replications, 4 treatments, and a plot size of 6 × 8 m with 2 m buffers between plots. A 1 × 1 m white marker card was placed outside the stake at each corner and georeferenced with an SXblue Platinum GPS device. Treatments consisted of (1) MB control and BB control, (2) MB but no BB control, (3) no MB control but BB control, and (4) untreated control (i.e., no Monilinia or Botrytis blight prevention treatments). Despite this design, the experimental approach adopted in this study may not conform to every location; thus, other treatment options have been explored. Similar experimental designs have focused on using

treatments such as nitrogen fertilization when monitoring the growth and development of plants [8]. Notwithstanding, the experimental design and treatments should be compatible with the wild blueberry plant type. Furthermore, since the growth and development of the plant is influenced by both biotic (disease infestation) and abiotic factors (nutrients and environmental conditions), continuous monitoring is required.

2.3. Fungicide Application

Fungicides were applied to the treatment plots as described by Anku et al. [18]. The experimental design was intended not to study the effects of fungal control products on MB and BB but rather to stimulate variation and the natural occurrence of these diseases for analysis.

2.4. Data Acquisition

2.4.1. Field Data Collection on Growth Parameters

Fifteen (15) stems per plot were simultaneously collected as aerial imagery was acquired. These collections were conducted from the F0/F1 stage until the F8 stage (fruit set; Table 1). The stems were collected diagonally at 20 cm intervals along a 4 m line transect, cutting the stem as close to the base as possible to avoid vegetative stems [23]. Growth parameters taken from each plot included plant height (PH), vegetative node number (VN) and stage (VS), floral node number (FN) and stage (FS), leaf area index (LAI; measured with an SS1 SunScan Canopy Analysis System, Delta-T Devices), and harvestable yield. Harvestable yield was collected in August 2020 with a forty-tine commercial wild blueberry hand rake from six randomly selected 1 m^2 quadrats in each plot [23].

Table 1. Flight details conducted at the Lemmon Hill and Kemptown locations at the different phenological stages.

Flight Date	Plant Stage	MicaSense RedEdge Camera	
		30 m	Spatial Resolution (cm/px)
20 May 2020	F1 (Bud break)	✓	2.2
2 June 2020	F2/F3 (Tight cluster)	✓	2.2
10 June 2020	F4/F5 (Early/late bud)	✓	2.2
18 June 2020	F6/F7 (Bloom)	✓	2.2
26 June 2020	F8 (Fruit set)	✓	2.2

2.4.2. Multispectral Platform and Aerial Image Acquisition

The DJI Matrice 600 Pro UAV (a DJI product, Shenzhen, China) was equipped with a 5-band MicaSense RedEdge™-M multispectral camera (AgEagle, Wichita, KS, USA) (Figure 1B) to take images at these wavelengths: blue (475), green (560), red (668), red edge (717), and near-infrared (840) banded imagery. Using ground control points (GCPs) (Figure S1), the Matrice 600 Pro was flown at a 30 m height with a frontal image overlap of 75% and a side image overlap of 70%.

The imagery was acquired within an interval of 8 to 13 days (depending on weather conditions) for a total of 5 flights. Image collection was conducted under clear conditions to minimize the effects of clouds, wind, and rain. Calibration and adjustments were carried out to minimize the effects of distortion on the quality of imagery obtained. All imagery was acquired at a 2.2 cm spatial resolution (Table 1).

2.4.3. Postprocessing and Extraction of Vegetation Indices

Imagery acquired from the multispectral camera was processed into a composite orthomosaic image using a web processing tool, Solvi (https://solvi.ag/features, accessed on 15 April 2022 which was previously owned by Precision Hawk) [18]. Individual plots were digitized, and their vegetation indices were extracted. The extracted file was exported as a comma-separated-value (CSV) file into Excel for further arrangement and processing. ArcGIS version 10.5 was further used to digitize and process some of the images as shown in the workflow (Figure 2).
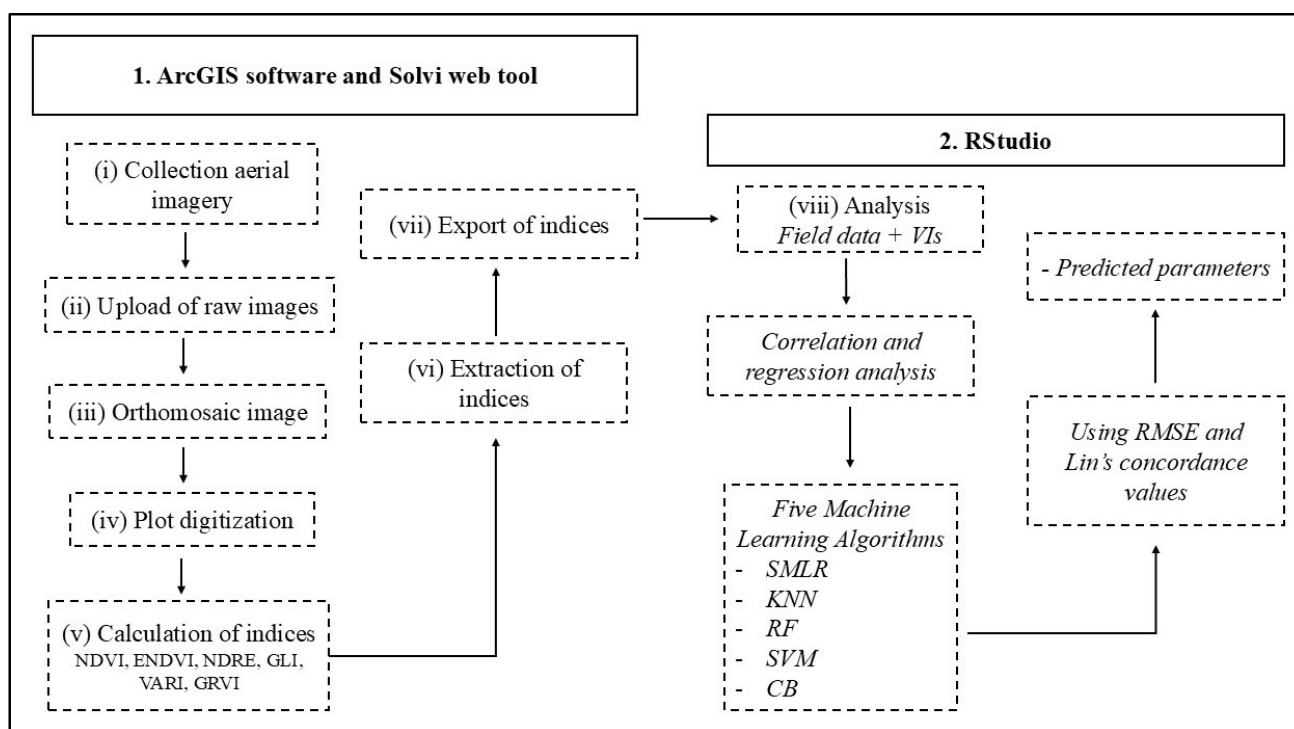

Figure 2. General overview of the workflow for the postprocessing of aerial images.

2.5. Vegetative Indices

VIs computed using light bands perform several functions in plants, including monitoring and prediction, among other functions. Three of these VIs, NDVI, ENDVI, and NDRE, use the near-infrared (NIR) band, with the other three restricted to the visible light region (VIS) (Table 2).

Table 2. Vegetative Indices Used in This Study.

Vegetation Indices	Bands [a]	Equation [b]
Green Leaf Index (GLI)	R, G, B	$(2 \cdot R_g - R_r - R_b)/(2 \cdot R_g + R_r + R_b)$
Green, Red Vegetation Index (GRVI)	R, G	$(R_g - R_r)/(R_g + R_r)$
Normalized Difference Vegetation Index (NDVI)	R, NIR	$(R_n - R_r)/(R_n + R_r)$
Enhanced Normalized Difference Vegetation Index (ENDVI)	B, G, NIR	$(R_n + R_g) - (2*R_b)/(R_n + R_g) + (2*R_b)$
Normalized Difference Red Edge (NDRE)	NIR RE	$(R_n - R_{re})/(R_n + R_{re})$
Visible Atmospheric Red Index (VARI)	G, R	$(1 + 0.5) (R_n - R_r)/(R_n + R_r + 0.5)$

[a] Indices were grouped based on the major wavelengths of the MicaSense sensor: NIR (n, 840 nm), red edge of chlorophyll absorption (RE, 717 nm), red (R, 668 nm), green (G, 560 nm), blue (B, 475 nm). [b] R is the reflectance at wavelength; R_n, R_{re}, R_r, R_g, and R_b are the reflectance for the NIR, RE, red, green, and blue bands, respectively.

2.6. Statistical Analysis and Regression Methods

Correlation and regression analysis were used to establish the relationship between VIs and the different growth parameters in the combined data set. The correlation method focused on establishing the strength of the relationship between the two quantitative (dependent and independent) variables. The regression method then described the relationship between the variables [24]. Therefore, machine learning, using the supervised regression approach, was utilized. The supervised machine learning regression method allows the system to model the relationship between the response and dependent variables after training the machine. This gives the machine learning method a predictive ability. Despite using other methods such as the coefficient of determination value (R^2), recent studies have adopted Lin's concordance correlation coefficient (CCC) as a higher measure of accuracy and precision. The CCC measures how far the linear relationship of the two variables deviates from the concordance line (accuracy) and how far each observation also deviates from the fitted line (precision) [25–27]. The correlation and regression analysis and Lin's concordance correlation coefficient (CCC) analysis were performed using the R software, version 4.2.0.

In this study, stepwise multiple linear regression was used as a fundamental technique to select a subset of useful independent variables and evaluate the order of importance of these variables [28,29]. The support vector machine (SVM) was also used in this study as a linear binary classifier that identifies a single boundary between two classes by finding a hyperplane that separates the dataset using predefined training data [30]. This study also adopted the random forest (RF), a supervised ML classifier based on decision trees primarily used for classification and regression tasks [31]. This study also used a K-nearest neighbor algorithm. This algorithm is used for classification and regression tasks based on finding the k nearest data points to a given query point [32]. Lastly, cubist regression was adopted. Cubist regression is a machine learning regression technique that is rule-based; thus, it combines decision trees and linear regression. These classifiers were chosen for their effectiveness with small datasets and their ability to manage overfitting, handle missing values, deal with high-dimensional data and outliers, accommodate complex relationships, and ensure model robustness [33,34].

Therefore, this study modified the approach of Yu et al. [35] by conducting these analyses using five (5) machine learning algorithms, stepwise multilinear regression (SMLR), K-nearest neighbor (KNN), random forest (RF), support vector machine (SVM), and the cubist method (CB), to identify which method constructed the best regression relationship. These classifiers were set up using a 10-fold cross-validation approach and were repeated 10 times. In addition to the R^2, CCC, and RMSE values in determining growth parameters, output or results from the analysis also facilitated the generation of variable importance plots.

A variable importance chart was produced, and this determined the overall impact of each VI, with the most significant VI having the most predictive power. To differentiate between the two groups of vegetation indices, we determined which group (VIS and NIR vegetation indices) had the highest predictive power. This was achieved by sampling the top three VIs from all regression analyses to determine individual VI contributions in achieving those predictions. The analysis generated from the R software presented ranked contributions of the individual VIs on a scale of 0–100%, where 100% represented a high contribution and 0% indicated a low contribution. These contributions were evaluated by selecting the top 3 highest-ranking VIs within a specific phenological stage as the most significant VIs. This approach facilitated the identification of the VI with the most predictive ability for a given parameter as determined by the regression algorithm. This method was a simplified and modified version of what was adopted by Souza et al. [36]. After identifying the 3 best VIs (with an average of between 60% to 91%) across all phenological stages for

the different classifiers, their occurrences in the first, second, and third positions of these VIs were counted. The VI with the highest number of appearances in these positions was considered the overall most influential vegetative index in the generated results.

3. Results

3.1. Correlations Between VIs and Growth Parameters

Correlation analysis between VIs and growth parameters showed moderately high, significant values (Figure 3). However, these values were inconsistent among the different parameters and phenological stages. The results indicated that VIs can be used to determine and potentially make predictions on different plant parameters in the wild blueberry fields.

Among the different phenological stages, correlation values were generally low at the bud break (F1) and the fruit set stages (F8) (Figure 3A,E). However, LAI and vegetative bud number (VN) gave high correlation values under the NIR indices. At the tight cluster stage, high correlations were observed among VIs, PH, and LAI (Figure 3B). While the NIR indices showed a high correlation with yield, the visible light vegetative indices (VIS) showed a good correlation with vs (Figure 3B). The tight cluster stage showed high correlation values among some VIs, PH, FS, VS, and yield (Figure 3C). Among these values, ENDVI was inconsistent with FS, VS, and yield. The bloom stage was characterized by high correlation values occurring at PH, FS, VN, and LAI (Figure 3C). LAI observed very high values across the different index types, with PH and VN.

Correlating with the VIS indices while FS correlated with the NIR indices. NDVI showed a high correlation with yield and VN (Figure 3D). The fruit set stage was characterized by the lowest correlation among the different phenological stages. Only ENDVI showed a good positive correlation with yield (Figure 3E). Generally, the tight cluster, early/late bud, and fruit set stages observed significant correlation values between growth parameters and VIs. GLI, GRVI, and VARI were consistent in generating moderately high r values for the tight cluster, early/late bud, and flowering stages, whereas NDVI, ENDVI, and NDRE were consistent at the tight cluster and early/late bud stages. This trend points to the relevance of some visible-light-generated VIs, which performed slightly better in some parameters than the near-infrared VIs.

Variable importance enabled the determination of VIs that had the most predictive power. Variables with high importance value were drivers of the outcome; thus, their values significantly affected the overall outcome (Figures 4 and 5). This analysis revealed that the NIR indices contributed significantly to the outcomes observed, with some contribution from the VIS vegetative indices (Tables 3, 4 and S1A,B). For LAI under all phenological stages, NDVI, NDRE, and ENDVI contributed significantly. FN and FS observed significant contributions from GRVI, VARI, ENDVI, and NDRE. PH, VS, and VN were significantly impacted by VIs such as NDRE, NDVI, ENDVI, and GRVI under all phenological stages. Sampling some of the highest VIs of every parameter under a specific classifier of a variable importance output implied that, despite the contribution from the NIR indices, the VIS vegetative indices cannot be underestimated, as they contributed significantly to major outcomes observed (Tables 3–5 and S1A,B). Representation on rankings was considered for only four classifiers, excluding the cubist classifier, which had low or no represented results.
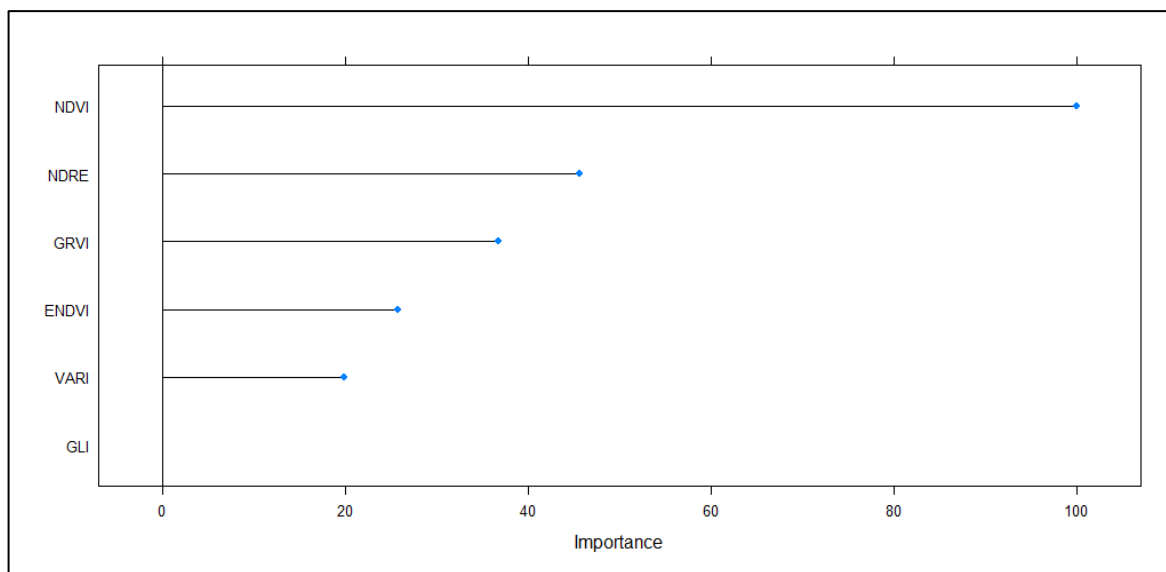
Figure 3. Correlation coefficients between growth parameters and VIs using the multispectral sensor at the different phenological stages. (**A**) F1 stage (bud break), (**B**) F2/F3 stage (tight cluster), (**C**) F4/F5 stage (early/late bud), (**D**) F6/F7 stage (bloom), and (**E**) F8 stage (Fruit set). Color intensities indicate the degrees of positive and negative correlation values.

Figure 4. A variable importance chart of the random forest algorithm at the F6/F7 stage representing the contributions of individual VIs to the observed output.
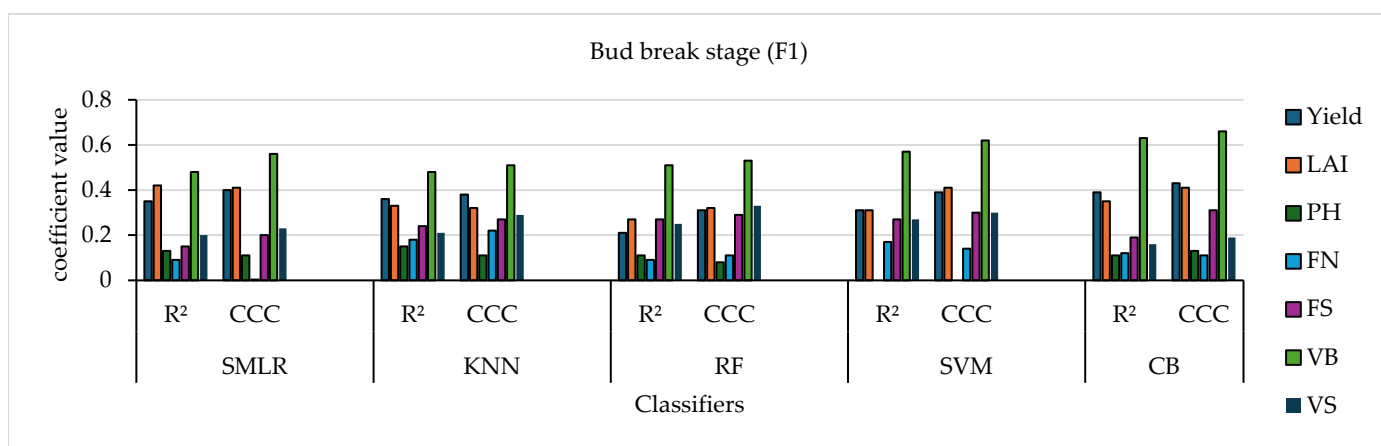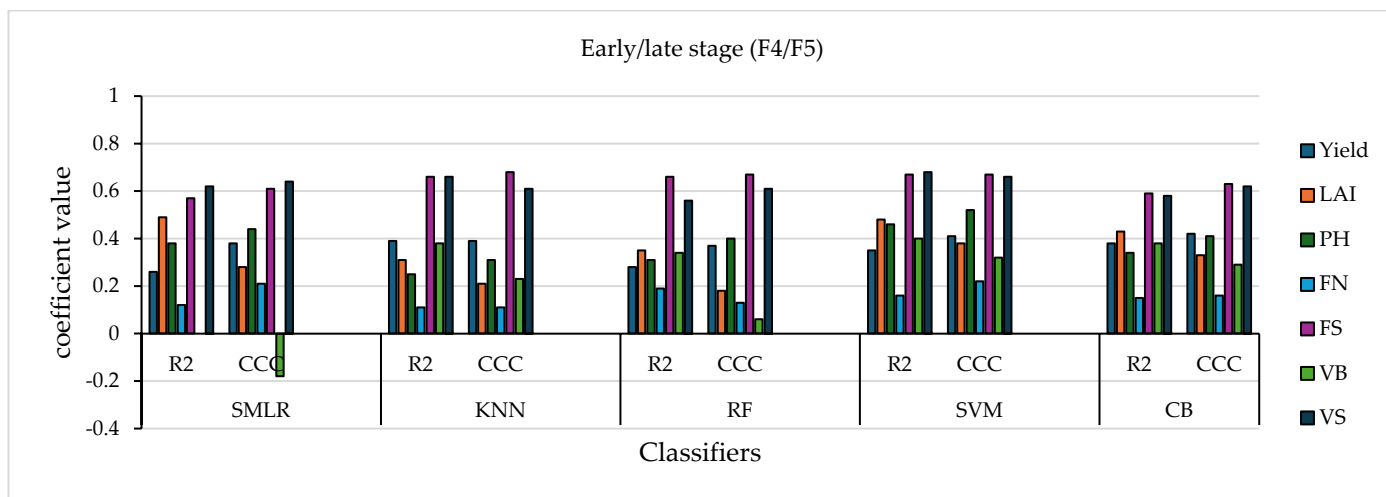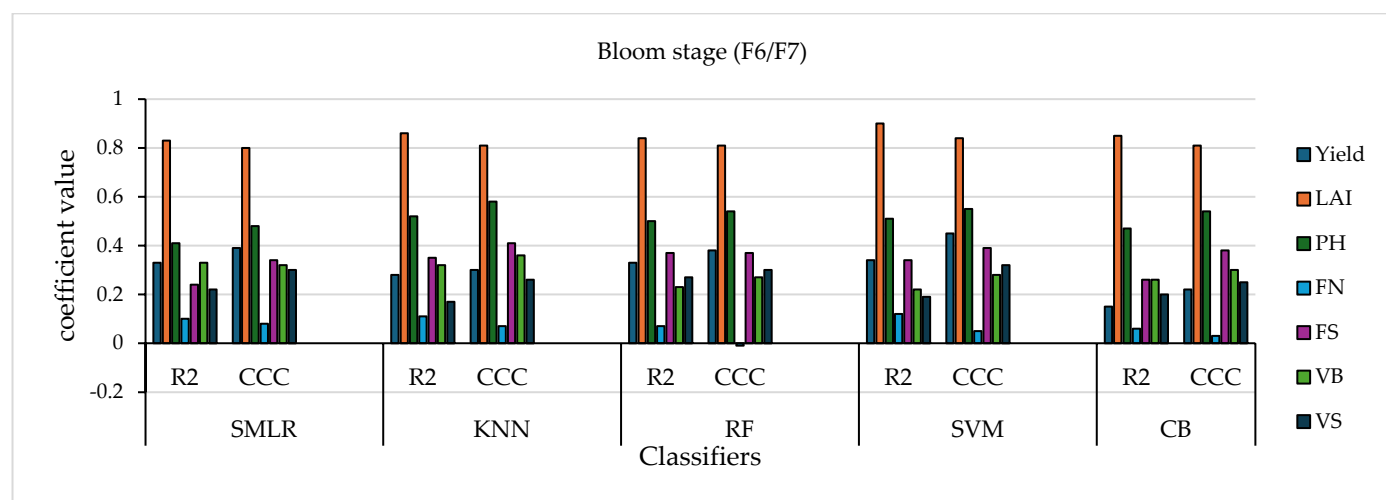

(**a**)
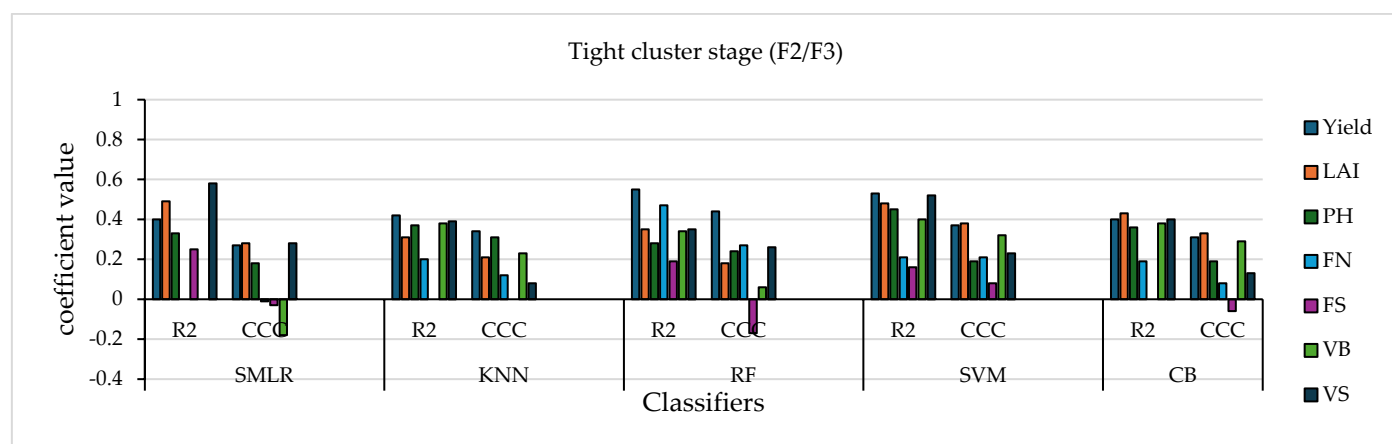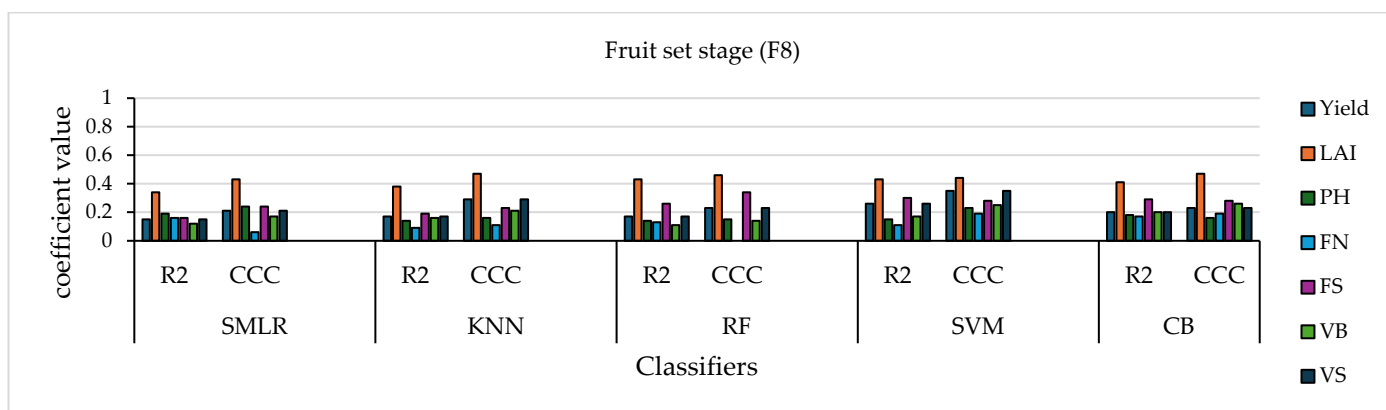

(**b**)

Figure 5. *Cont.*

(**c**)

(**d**)

(**e**)

Figure 5. Coefficient of determination (R^2) values and Lin's concordance (CCC) values from 5 regression methods on several growth parameters against VIs at the different phenological stages (**a**–**e**) using the multispectral sensor. SMLR—stepwise multilinear regression, KNN—k-nearest neighbor, RF—random forest, SVM—support vector machine, CB—cubist, F—floral stage, Yield—harvestable yield, LAI—leaf area index, PH—plant height, FN—floral bud number, FS—floral stage, VB—vegetative bud number, and VS—vegetative bud stage.

3.2. Predicting Growth Parameters Using Vegetative Indices

Coefficient of determination (R^2) values showed high significant values among some parameters at the different phenological stages (Figure 5a–e; Tables 3, 4 and S1A,B). Regression analysis estimated moderately high R^2 values among all the regression methods of analysis.

A range of R^2 values with relatively low RMSE values were observed among some growth parameters, such as LAI (Figure 5a–e and Table 3). However, this observation was consistent only for LAI at all phenological stages while being restricted to the F4/F5 stage for FS and VS. Despite the relatively low values observed by LAI at the bud break, tight cluster, and early/late bud stages, LAI recorded the highest R^2 values at the bloom stage, with an average of about 45–50% of RMSE (Figure 5d and Table 3). With the R^2, CCC, and RMSE as selective criteria, it was observed that relatively high R^2 values were observed among some parameters with moderate RMSE values (Table 3).

Table 3. Root means square error values (RMSE) for the R^2 and CCC values obtained from 5 regression methods on several growth parameters against VIs at the different phenological stages using the multispectral sensor. SMLR—stepwise multilinear regression, KNN—k-nearest neighbor, RF—random forest, SVM—support vector machine, CB—cubist, F—floral stage.

Parameters	Bud break stage (F1)				
	SMLR	KNN	RF	SVM	CB
Yield (g.m^{-2})	225.85	223.83	249.73	240.11	223.86
LAI	0.11	0.12	0.12	0.11	0.11
Plant height (cm)	1.59	2.13	1.71	-	1.79
Floral bud no.	1.61	1.72	1.46	1.64	1.58
Floral bud stage	0.26	0.25	0.24	0.25	0.26
Veg. bud no.	3.17	3.32	3.14	2.77	2.75
Veg. bud stage	0.25	0.23	0.24	0.24	0.25
	Tight cluster stage (F2/F3)				
Yield (g.m^{-2})	340.10	273.35	266.10	333.75	372.77
LAI	0.11	0.13	0.13	0.11	0.12
Plant height (cm)	2.12	1.94	1.90	1.85	1.86
Floral bud no.	1.45	1.98	1.34	1.63	1.36
Floral bud stage	0.69	0.53	0.67	0.91	0.56
Veg. bud no.	3.08	2.59	2.64	2.37	2.23
Veg. bud stage	0.81	0.89	0.86	0.80	0.91
	Early/late stage (F4/F5)				
Yield (g.m^{-2})	230.12	224.70	240.80	224.27	221.05
LAI	0.11	0.14	0.13	0.11	0.12
Plant height (cm)	1.88	1.99	1.94	1.76	1.99
Floral bud no.	1.50	1.59	1.55	1.48	1.57
Floral bud stage	0.52	0.47	0.46	0.47	0.49
Veg. bud no.	3.08	2.59	2.64	2.37	2.23
Veg. bud stage	0.32	0.32	0.33	0.29	0.31
	Bloom stage (F6/F7)				
Yield (g.m^{-2})	232.24	254.21	232.13	224.38	264.94
LAI	0.56	0.56	0.54	0.46	0.55
Plant height (cm)	1.45	1.41	1.37	1.32	1.38
Floral bud no.	1.08	1.03	1.17	1.08	1.13
Floral bud stage	0.14	0.12	0.13	0.12	0.13
Veg. bud no.	1.54	1.43	1.53	1.66	1.56
Veg. bud stage	0.21	0.28	0.22	0.33	0.25

Table 3. *Cont.*

	Fruit set stage (F8)				
Yield (g.m^{-2})	265.70	304.26	249.36	235.18	265.63
LAI	0.90	0.83	0.87	0.87	0.89
Plant height (cm)	2.05	2.00	2.14	2.88	2.19
Floral bud no.	1.05	1.00	1.08	1.11	1.05
Floral bud stage	-	-	-	-	-
Veg. bud no.	2.07	2.05	2.15	1.97	2.02
Veg. bud stage	0.17	0.20	0.17	0.17	0.18

3.3. Phenological Growth in the Fields

The trend of VI measurements using the UAV multispectral sensor was similar at the two locations. The UAV measurements clearly illustrated that the NIR VIs were separated from the VIS vegetative indices, except for NDRE (Figure 6). At both locations, NDVI and ENDVI obtained the highest VI values with a >100% and a 60.6% increase at harvest, respectively, compared with the other indices across the phenological stages. NDRE at the Kemptown and Lemmon Hill locations observed a 67.9% and a 51.7% increase in VI value at harvest, respectively. The VIS vegetative index from both locations progressed from the negative quadrant into the positive quadrant, with increases of over 100% in VI values for all three indices (GLI, GRVI, and VARI), with VARI being the highest. From both fields, VARI performed best among the three (3) VIS vegetative indices, followed by GLI and then GRVI at all phenological stages (Figure 6). Interestingly, VARI observed continuous growth until an almost equal value was observed with NDVI and ENDVI at the Kemptown field site, giving it the highest increase in VI value at harvest compared with the initial bud break value. Though a similar effect of VARI was not seen at Lemmon Hill, it observed the highest increase compared with the other VIS indices. All VIs observed a varying degree of decline at the bloom stage.
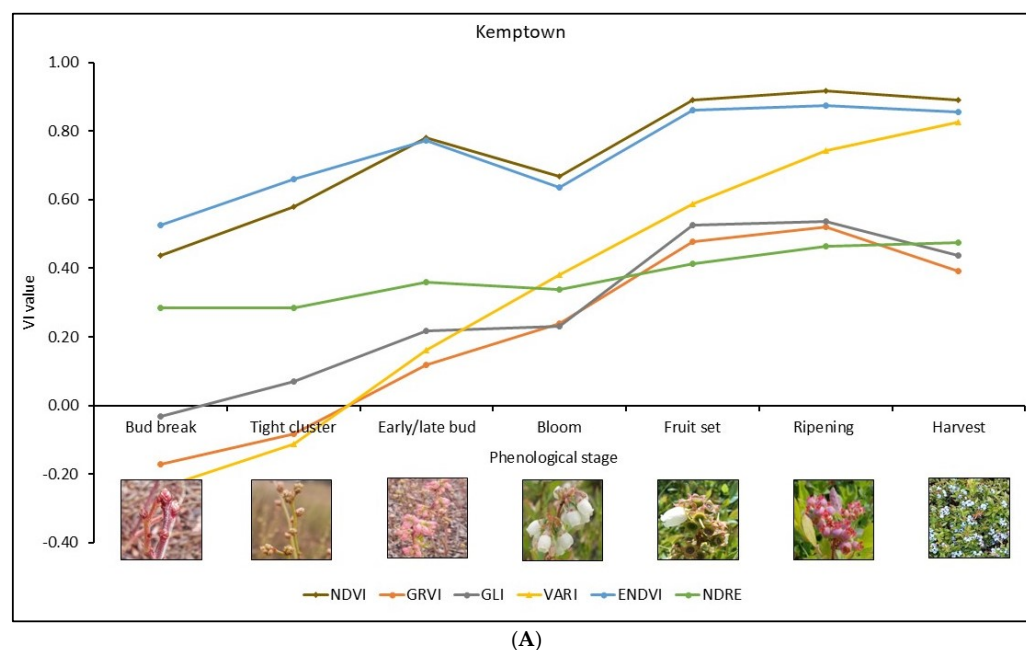

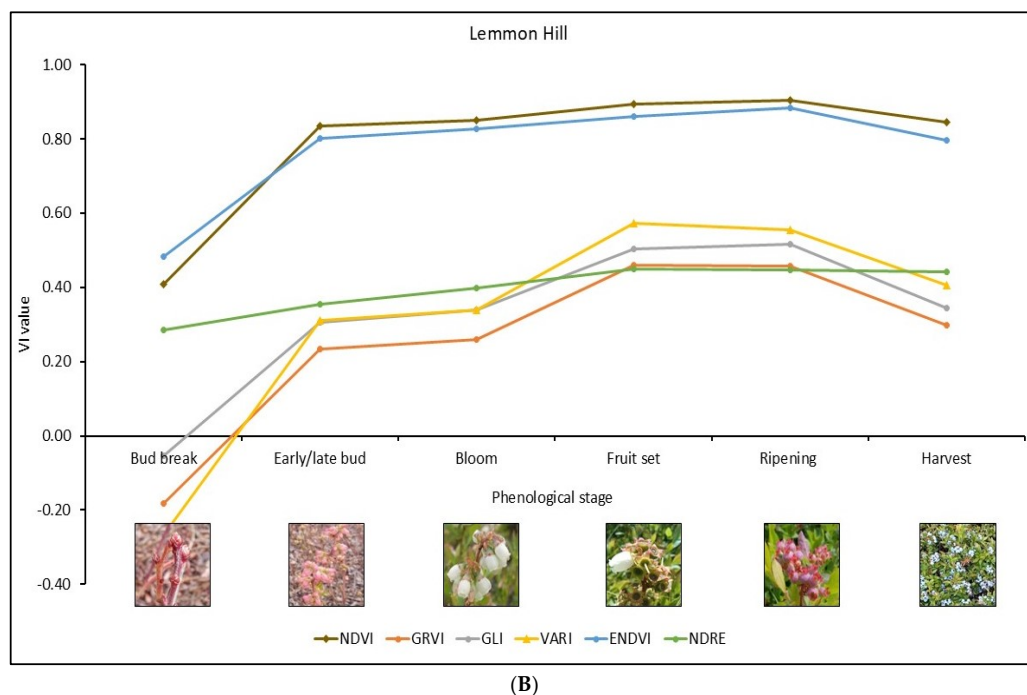(**A**)

Figure 6. *Cont.*

(B)

Figure 6. The growth progression of VIs observed in both fields at the different phenological stages using the multispectral sensor. (**A**) Kemptown and (**B**) Lemmon Hill.

3.4. Variable Importance Plot

A performance ranking of the vegetative indices (VIs) was conducted by selecting the top three highest VIs from the variable importance plots (Tables 4, 5 and S1A,B). Significant contributions were observed from the light-based VIs, particularly GLI, GRVI, and VARI. Notably, GLI appeared 24 times in a first-place position in the variable importance plots (Table 5), making it the most predictive vegetative index. Following GLI was ENDVI appearing 22 times, with both NDRE and GRVI appearing 20 times, in third-placed position. In second-place positions, VARI was the most prominent, followed by GRVI and NDVI. Similarly, in the third-place positions, GLI was the most prominent, followed by NDVI and NDRE (Table 5).

Table 4. Rankings on an SVM classifier for the best-performing indices for each phenological stage and parameter using the multispectral sensor. Performance was evaluated using outputs from the variable importance chart. Percentages represent the performance of the individual vegetative indices in achieving that outcome. Indices are arranged in order from the best index to the least performing index along with their corresponding percentages.

Bud break stage (F1)		
Parameter	**Rank**	**Percentage (%)**
Yield (g.m^{-2})	GLI, VARI, GRVI, NDRE, NDVI, ENDVI	100, 75,60, 25, 10, 0
Leaf area index	NDRE, NDVI, ENDVI, GLI, GRVI, VARI	100, 90, 80, 10, 5, 0
Plant height (cm)	NDRE, NDVI, ENDVI, GRVI, VARI, GLI	100, 95, 75, 68, 28, 0
Floral bud number	NDRE, NDVI, ENDVI, GRVI, VARI, GLI	100, 75, 70, 45, 15, 0
Floral bud stage	GLI, VARI, GRVI, NDRE, ENDVI, NDVI	100, 90, 88, 82, 30, 0
Vegetative bud number	ENDVI, NDVI, NDRE, VARI, GRVI, GLI	100, 70, 18, 3, 2, 0
Vegetative bud stage	GLI, VARI, GRVI, NDRE, ENDVI, NDVI	100, 88, 82, 30, 5, 0

Table 4. *Cont.*

Tight cluster stage (F2/F3)		
Parameter	**Rank**	**Percentage (%)**
Yield (g.m^{-2})	GRVI, NDRE, NDVI, VARI, ENDVI, GLI	100, 80,75, 70, 45, 0
Leaf area index	GRVI, VARI, GLI, ENDVI, NDRE, NDVI	100, 70, 45, 20, 14, 0
Plant height (cm)	NDRE, NDVI, ENDVI, VARI, GLI, GRVI	100, 95, 80, 5, 5, 0
Floral bud number	GRVI, VARI, NDRE, GLI, NDVI, ENDVI	100, 85, 30, 15, 10, 0
Floral bud stage	GLI, GRVI, VARI, ENDVI, NDRE, NDVI	100, 90, 78, 45, 23, 0
Vegetative bud number	ENDVI, NDRE, NDVI, GLI, VARI, GRVI	100, 68, 50, 48, 12, 0
Vegetative bud stage	GLI, VARI, GRVI, ENDVI, NDVI, NDRE	100, 92, 83, 24, 18, 0

Early/late bud stage (F4/F5)		
Parameter	**Rank**	**Percentage (%)**
Yield (g.m^{-2})	VARI, GRVI, GLI, NDVI, NDRE, ENDVI	100, 100,100, 90, 70, 0
Leaf area index	GRVI, VARI, GLI, ENDVI, NDRE, NDVI	100, 70, 45, 20, 15, 0
Plant height (cm)	ENDVI, NDVI, NDRE, GLI, GRVI, VARI	100, 78, 50, 40, 30, 0
Floral bud number	GLI, GRVI, ENDVI, NDVI, NDRE, VARI	100, 65, 55, 45, 18, 0
Floral bud stage	GRVI, VARI, GLI, NDVI, NDRE, ENDVI	100, 95, 93, 65, 45, 0
Vegetative bud number	ENDVI, NDRE, GRVI, DNVI, GLI, VARI	100, 63, 23, 22, 12, 0
Vegetative bud stage	VARI, GRVI, GLI, NDVI, NDRE, ENDVI	100, 100, 98, 80, 72, 0

Bloom stage (F6/F7)		
Parameter	**Rank**	**Percentage (%)**
Yield (g.m^{-2})	GLI, ENDVI, NDVI, GRVI, NDRE, VARI	100, 95,80, 80, 50, 0
Leaf area index	NDRE, NDVI, ENDVI, GLI, GRVI, VARI	100, 100, 90, 80, 25, 0
Plant height (cm)	ENDVI, NDVI, NDRE, GLI, GRVI, VARI	100, 78, 50, 40, 30, 0
Floral bud number	NDRE, GRVI, NDVI, GLI, VARI, ENDVI	100, 98, 82, 70, 50, 0
Floral bud stage	ENDVI, NDRE, NDVI, GLI, GRVI, VARI	100, 95, 82, 58, 25, 0
Vegetative bud number	GLI, GRVI, NDRE, NDVI, ENDVI, VARI	100, 82, 68, 50, 32, 0
Vegetative bud stage	ENDVI, GLI, GRVI, VARI, NDRE, NDVI	100, 78, 55, 38, 15, 0

Fruit set stage (F8)		
Parameter	**Rank**	**Percentage (%)**
Yield (g.m^{-2})	ENDVI, NDRE, NDVI, GRVI, GLI, VARI	100, 90,80, 75, 50, 0
Leaf area index	GRVI, VARI, GLI, NDVI, ENDVI, NDRE	100, 95, 92, 35, 23, 0
Plant height (cm)	GRVI, VARI, GLI, ENDVI, NDRE, NDVI	100, 85, 80, 8, 4, 0
Floral bud number	NDVI, GLI, NDRE, VARI, GRVI, ENDVI	100, 75, 70, 50, 15, 0
Floral bud stage	NDRE, GRVI, VARI, NDVI, ENDVI, GLI	100, 58, 50, 40, 7, 0
Vegetative bud number	GRVI, VARI, GLI, ENDVI, NDVI, NDRE	100, 90, 88, 70, 25, 0
Vegetative bud stage	GLI, ENDVI, GRVI, NDVI, VARI, NDRE	100, 95, 45, 35, 11, 0

Table 5. Overall rankings of the best performing VIs at the different phenological stages. Performance evaluation was based on the variable importance plot. Numbers indicate the number of appearances in each position, indicating the performance index of each phenological stage.

VI	Positions	Bud Break (F1)	Tight Cluster (F2/F3)	Early/Late Bud (F4/F5)	Bloom (F6/F7)	Fruit Set (F8)	Best Performance
	1st	9	4	3	4	4	24
GLI	2nd	1	2	-	3	4	10
	3rd	-	2	11	1	7	21
	1st	-	6	6	1	7	20
GRVI	2nd	-	4	7	6	5	22
	3rd	6	3	2	2	4	17
	1st	-	3	5	2	2	12
VARI	2nd	7	5	6	-	8	26
	3rd	3	4	2	1	5	15

Table 5. *Cont.*

VI	Positions	Bud Break (F1)	Tight Cluster (F2/F3)	Early/Late Bud (F4/F5)	Bloom (F6/F7)	Fruit Set (F8)	Best Performance
NDVI	1st	2	1	-	2	2	7
	2nd	8	3	4	4	-	19
	3rd	2	5	1	9	2	19
ENDVI	1st	3	3	6	7	3	22
	2nd	4	1	1	2	2	10
	3rd	8	3	2	3	1	17
NDRE	1st	7	4	1	5	3	20
	2nd	1	6	3	6	2	18
	3rd	3	5	3	5	2	18

Despite the individual rankings, it was observed that, collectively, the light VIs were prominent at the tight cluster, early/late bud, and fruit set stages. Conversely, the NIR VIs were significant at the bud break and bloom stages. Nevertheless, both types of vegetative indices contributed significantly to the predictions observed (Table 5).

3.5. Assessment of Statistical Methods

The five adopted statistical classifiers performed similarly, with consistent values across different methods applied to the parameters. Despite the slight differences in the statistical approaches of these classifiers, they were consistent in their output values. The support vector machine (SVM) generally had high output values across all phenological stages, which were often consistent with the random forest (RF) method. The stepwise multiple linear regression (SMLR) method was also consistent with the K-nearest neighbor (KNN) method, with the cubist method (CB) considered slightly different from the other four (4) methods. However, the general difference in result output observed between these methods was not substantial.

A comparison between the coefficient values using R^2 and CCC (Figure 5a–e; Tables 3 and 4) illustrated great similarity. Apart from the tight cluster stage and bloom stage (Figure 5b and Table 3), all the remaining phenological stages observed consistently higher coefficient values using CCC than the R^2 values (with a few exceptions, e.g., early/late bud stage—LAI) (Figure 5a,c–e and Table 3). Therefore, slightly higher coefficient values were observed using CCC across the different phenological stages (Figure 5a–e and Table 3).

4. Discussion

The trend in VI demonstrated the phenological growth over the measured period, confirming the use of VIs to monitor phenology [12,13,15]. Findings from this study confirmed that plant canopy and VIs showed a bell-like-shaped representation over the field season [12]. Therefore, VI values were low at the beginning of the crop season, increased midway, and diminished at the end of the season. This observation was consistent with the study of Forsström et al. [12] regarding the general growth and development of plants. Their work observed a similar occurrence when comparing lingonberry and blueberry spectra. This phenomenon was due to leaf development over the growing period, which continued until the autumn season, when chlorophyll and other pigments were degraded, and leaves fell from the stem. The bell-shaped representation suggests that plant leaves are major determinants of VIs and regulators of light, with pigment contributing to this process. This result agreed with the work of Souza et al. [8], who observed a similar occurrence with the phenological indices in cotton. This observation gives insight into the phenological cycle of the wild blueberry plant (leaves), highlighting specific phenological stages for management practices. Leaves, being the primary drivers of photosynthesis, are critical

for growth and can serve as indicators for forecasting plant health and diseases such as Monilinia and Botrytis blossom blight.

After the bud break stage, it was observed that the increasing trend of VIs was disrupted at the flowering stage, where several VIs exhibited a moderate to severe decline. This phenomenon was confirmed by the work of Hassan et al. [7], who reported a 10% decline in VIs at the flowering stage. This decline was reflected in the Lemmon Hill field, with an even greater decline observed in the Kemptown field.

The reasons accounting for this decline may vary; however, field observations suggest that variations in VIs in the wild blueberry fields are strongly associated with the transition between phenological stages. Notably, the dominant field species, *V. angustifolium*, produces white corollas at the bloom stage, potentially affecting reflectance values and contributing to the observed decline.

Additionally, leaf structure and angle significantly influence light reflection captured by the MicaSense, which may have affected the computation of these VIs. Since wild blueberry plants are not evergreen, their leaves exhibit varying colorations at different phenological stages. Consequently, the presence of pink and white flowers along with the diverse coloration of leaves, creates a mosaic of colors in the field [18]. Furthermore, new flushes of vegetative growth after fruit set with the breaking of auxiliary buds and the emergence of new flushes of leaves also contribute to this variation. This occurrence was attributed to the chemical composition of leaves and the varied corollas along the early to middle stages of development significantly affecting reflectance [37,38]. Other contributing factors included the direction of incidence radiation and canopy architecture, among other characteristics of the plant playing a role in these observations [13]. The variability effect of phenotypes was also evident across fields. For example, during the bloom stage, Kemptown observed a general decline in VIs, whereas this effect was less pronounced in Lemmon Hill. This study largely confirms the findings of Forsström et al. [12], where variations in the red and blue wavelength regions accounted for the decline at the bloom and berrying stages of the plant [12]. Therefore, since VIs are computed from VIS and NIR light, this potentially accounts for the observed variations in this study. However, the seeming difference observed between the two fields stemmed from variations in the nature and quantity of leaves, flowers, and berries present in both fields. These differences, particularly at the transitioning phases, affect VIs at the different phenological stages [12]. Consistently with these findings, Forsström et al. [12] demonstrated that VIs are sensitive to blueberry shrub phenology observed throughout the growing season, underscoring the potential of using VIs to monitor phenology effectively.

The predictability of growth parameters using RS techniques relies on obtaining high correlative and regression values with minimal RMSE [7,8,16–18]. This study recorded a range of moderately high R^2 and CCC, values which agreed with the findings from other crops such as wheat [7], wild blueberry [18], and rapeseed [13], among others. Among the growth parameters, LAI demonstrated high predictability across various phenological stages, except at the F8 stage, while FS and VS were predictable mainly during the F4/F5 stage. This study suggests that LAI, VS, and FS are growth parameters that can be estimated at different phenological stages across the field season. This conclusion aligns with the findings of Maqbool et al. [19], who used optimum multiple narrow-band reflectance (OMNBR) indices to estimate LAI at the bloom stage in wild blueberry fields. These findings corroborate our result that the bloom stage (F6/F7) is the optimal phenological stage for estimating LAI. Converse to our assertion on yield, a previous study by Maqbool et al. [19] indicated that yield can be predicted using reflectance data. Despite the seemingly different approach adopted by Maqbool et al. [19], the use of VIs may support the predictability of yield if measures are taken to rectify some issues on resolution, and specific harvest time.

Maqbool et al. [19] argued that the polyphenolic compounds contained in flowers and berries, compounded by the high variability levels present on the field, influenced spectral resolution and accurate estimations. Therefore, the inconsistencies observed with some of the results may directly point to field variability, which includes plant density across the field, different phenotypes, and the varying pigment composition of plants, affecting VIs. Findings on rapeseed and rice crops have pointed to the elongation and flowering stages as good estimation points for plant canopy and other biophysical characteristics. Similarly, as in this work, the optimal estimation stage for LAI is the bloom stage (white tip) (F6/F7), with early/late bud as the optimal estimation stage for both FS and VS. In the conclusions drawn by Lui et al. [16] and Zhou et al. [17], it was stated that VIs that show high correlation and prediction of LAI can also correlate and predict yield. While this assertion is partially supported by our study, with yield predictions showing high R^2 and CCC values under the RF and SVM models (Figure 5b), the high RMSE values implied high errors and low precision. The yield results from this study confirmed the results of MacEachern et al. [22] and Barai et al. [20]. Thus, to improve R^2 and RMSE values, it may be beneficial to harvest entire plots instead of relying on quadrant sampling. This approach would provide the total yields for individual treatment plots, enabling more accurate and effective analysis. On the selection of important VIs (variable importance), several vegetative indices (VIs) contributed to the varied outcomes observed in the use of the MicaSense multispectral sensor (Tables 4 and 5; Table S1A,B). Rather than a single linear regression method focusing on a specific index, multiple linear regression was adopted, and as such, several significant VIs showed their contributions to the values obtained. This result agreed with Yue et al. [39], whose work found superior the use of multiple indices rather than a single index to estimate crop parameters. Despite the advantages that the multiple index approach presents, other studies have pursued single-index assessment [12,18,20]. Though single-index assessment allows exploring the capabilities of a single index, it loses the ability to effectively compare those index values with other indices. Notably, the NIR indices such as NDVI, ENDVI, and NDRE contributed immensely across several parameters and growth stages with higher chances of effect [12]. However, the contribution of some light vegetative indices cannot be underestimated, and as such, this study makes a strong case for the VIS-VIs. Several studies have established that VARI, among other visible light VIs, estimates and monitors several growth parameters [11,16,17,40]. This agreed with Viña et al. [40] and Forsström et al. [12], who identified the visible atmospherically resistance index (VARI) and plant senescence reflectance index (PSRI), respectively, as good in monitoring phenology. The use of the different statistical classifiers was necessary to determine a suitable classifier. The classification methods applied proved robust; however, the results obtained varied slightly depending on the use of the R^2 and CCC approaches. In essence, both methods generated similar values and may be considered the same. In this study, the results obtained indicate that the SVM, RF, and CB classifiers generated high but similar values with minimal deviations between them.

Effective wild blueberry management practices are crucial in improving disease control, optimizing pollinator activity, and maximizing crop yields. Similarly, the ability to predict the number and developmental stage of floral buds provides insights into potential yields, allowing for early projections and better resource allocation. These advancements enable growers to manage key growth stages with greater precision, improving efficiency and productivity. The broader implication of this study lies in integrating these predictive capabilities into advanced decision-support models. By correlating plant growth dynamics with environmental conditions and VIs, these models can forecast disease spread, optimize the timing of pollinator release, and refine yield predictions. These tools help reduce costs, minimize environmental impacts, and promote sustainable farming practices [41]. Ultimately, the introduction of this

technique will empower growers to make data-driven decisions, enhancing productivity, profitability, and long-term stability in wild blueberry production.

5. Conclusions

This study assessed the potential of using the VIs to monitor and estimate growth and development parameters in the wild blueberry field. Results indicated the potential to adopt remote sensing as a valuable technological tool in the wild blueberry field. Correlative assessment of VIs against parameters showed good indication across all phenological stages. Results showed that LAI, FS, and VS can be estimated at the F4/F5 and F6/F7 stages, but yield prediction could be challenging, despite the potential shown.

The overall results from this study indicated that vegetative indices can be effectively used to generally monitor plant growth and make predictions. However, these determinations are specific to individual growth parameters. Therefore, using a well-established model, the introduction of VIs can help determine the LAI of the wild blueberry canopy. Notwithstanding the challenges observed in the other parameters, further research is required to validate the findings on harvestable yield. We recommend additional studies to compare the individual efficiencies of the VIS-VIs and the NIR-VIs. This comparison will help identify the potential of these index types in monitoring plant phenology. In addition, we recommend studies that would combine weather parameters to field and remotely sensed data to monitor phenology on the wild blueberry field.

References

1. Abbey, J.; Percival, D.; Asiedu, S.K.; Schilder, A. Susceptibility to Botrytis Blight at Different Floral Stages of Wild Blueberry Phenotypes. In Proceedings of the North American Blueberry Research and Extension Workers Conference, Orono, ME, USA, 12–15 August 2018.
2. Penman, L.N.; Annis, S.L. Leaf and Flower Blight Caused by *Monilinia vaccinii-corymbosi* on Lowbush Blueberry: Effects on Yield and Relationship to Bud Phenology. *Phytopathology* **2005**, *95*, 1174–1182. [CrossRef] [PubMed]
3. Abbey, J.A.; Percival, D.; Asiedu, S.K.; Prithiviraj, B.; Schilder, A. Management of Botrytis blossom blight in wild blueberries by biological control agents under field conditions. *Crop Prot.* **2020**, *131*, 105078. [CrossRef]
4. Fournier, M.-P.; Paré, M.C.; Buttò, V.; Delagrange, S.; Lafond, J.; Deslauriers, A. How plant allometry influences bud phenology and fruit yield in two Vaccinium species. *Ann. Bot.* **2020**, *126*, 825–835. [CrossRef] [PubMed]

5.   Krebs, C.J.; Boonstra, R.; Cowcill, K.; Kenney, A.J. Climatic determinants of berry crops in the boreal forest of the southwestern Yukon. *Botany* **2009**, *87*, 401–408. [CrossRef]

6.   Jones, C.L.; Maness, N.O.; Stone, M.L.; Jayasekara, R. Chlorophyll estimation using multispectral reflectance and height sensing. *Trans. ASABE* **2007**, *50*, 1867–1872. [CrossRef]

7.   Hassan, M.A.; Yang, M.; Rasheed, A.; Yang, G.; Reynolds, M.; Xia, X.; Xiao, Y.; He, Z. A rapid monitoring of NDVI across the wheat growth cycle for grain yield prediction using a multi-spectral UAV platform. *Plant Sci.* **2019**, *282*, 95–103. [CrossRef]

8.   Souza, H.B.; Baio, F.H.R.; Neves, D.C. Using passive and active multispectral sensors on the correlation with the phenological indices of cotton. *Eng. Agríc.* **2017**, *37*, 782–789. [CrossRef]

9.   Susmita, R. A Quick Review of Machine Learning Algorithms. In Proceedings of the International Conference on Machine Learning, Big Data, Cloud and Parallel Computing: Trends, Prespectives and Prospects: COMITCON-2019, Faridabad, India, 14–16 February 2019; p. 35.

10. El Naqa, I. , Li, R., Murphy, M.J. *Machine Learning in Radiation Oncology*; Springer International Publishing: Cham, Switzerland, 2015; ISBN 978-3-319-18304-6.

11. Anku, K.E.; Percival, D.C.; Rajasekaran, L.R.; Heung, B.; Vankoughnett, M. Remote estimation of leaf nitrogen content, leaf area, and berry yield in wild blueberries. *Front. Remote Sens.* **2024**, *5*, 1414540. [CrossRef]

12. Forsström, P.; Peltoniemi, J.; Rautiainen, M. Seasonal dynamics of lingonberry and blueberry spectra. *Silva Fenn.* **2019**, *53*, 10150. [CrossRef]

13. Hussain, S.; Gao, K.; Din, M.; Gao, Y.; Shi, Z.; Wang, S. Assessment of UAV-Onboard Multispectral Sensor for Non-Destructive Site-Specific Rapeseed Crop Phenotype Variable at Different Phenological Stages and Resolutions. *Remote Sens.* **2020**, *12*, 397. [CrossRef]

14. Zhang, J.; Wang, C.; Yang, C.; Xie, T.; Jiang, Z.; Hu, T.; Luo, Z.; Zhou, G.; Xie, J. Assessing the Effect of Real Spatial Resolution of In Situ UAV Multispectral Images on Seedling Rapeseed Growth Monitoring. *Remote Sens.* **2020**, *12*, 1207. [CrossRef]

15. Vega, F.A.; Ramírez, F.C.; Saiz, M.P.; Rosúa, F.O. Multi-temporal imaging using an unmanned aerial vehicle for monitoring a sunflower crop. *Biosyst. Eng.* **2015**, *132*, 19–27. [CrossRef]

16. Liu, T.; Li, R.; Zhong, X.; Jiang, M.; Jin, X.; Zhou, P.; Liu, S.; Sun, C.; Guo, W. Estimates of rice lodging using indices derived from UAV visible and thermal infrared images. *Agric. For. Meteorol.* **2018**, *252*, 144–154. [CrossRef]

17. Zhou, X.; Zheng, H.B.; Xu, X.Q.; He, J.Y.; Ge, X.K.; Yao, X.; Cheng, T.; Zhu, Y.; Cao, W.X. Predicting grain yield in rice using multi-temporal vegetation indices from UAV-based multispectral and digital imagery. *ISPRS J. Photogramm. Remote Sens.* **2017**, *130*, 246–255. [CrossRef]

18. Anku, K.E.; Percival, D.C.; Rajasekaran, L.R.; Heung, B.; Vankoughnett, M. Phenological assessment of the wild blueberry field using an unmanned aerial vehicle. *Acta Hortic.* **2023**, *1357*, 35–42. [CrossRef]

19. Maqbool, R.; Zaman, Q.; Percival, D.; Sharpe, S. Narrow Band Reflectance Measurements Can Be Used to Estimate Leaf Area Index, Flower Number, Fruit Set, and Berry Yield of the Wild Blueberry (*Vaccinium angustifolium* Ait.). *Acta Hortic.* **2010**, *926*, 363–369. [CrossRef]

20. Barai, K.; Tasnim, R.; Hall, B.; Rahimzadeh-Bajgiran, P.; Zhang, Y.-J. Is Drought Increasing in Maine and Hurting Wild Blueberry Production? *Climate* **2021**, *9*, 178. [CrossRef]

21. Paré, M.C.; Fournier, M.-P.; Lafond, J.; Deslauriers, A. How management practices influence vegetative and reproductive plant traits of wild lowbush blueberry species. *Can. J. Plant Sci.* **2022**, *102*, 1007–1015. [CrossRef]

22. MacEachern, C.B.; Esau, T.J.; Schumann, A.W.; Hennessy, P.J.; Zaman, Q.U. Detection of fruit maturity stage and yield estimation in wild blueberry using deep learning convolutional neural networks. *Smart Agric. Technol.* **2023**, *3*, 100099. [CrossRef]

23. Percival, D.; Beaton, E. Suppression of *Monilinia* Blight: Strategies for Today and Potential Fungicide Options for Tomorrow. *Int. J. Fruit Sci.* **2012**, *12*, 124–134. [CrossRef]

24. Liang, K.Y.; Zeger, S.L. Regression Analysis for Correlated Data. *Annu. Rev. Public Health* **1993**, *14*, 43–68. [CrossRef] [PubMed]

25. Crawford, S.B.; Kosinski, A.S.; Lin, H.-M.; Williamson, J.M.; Barnhart, H.X. Computer programs for the concordance correlation coefficient. *Comput. Methods Programs Biomed.* **2007**, *88*, 62–74. [CrossRef] [PubMed]

26. Kwiecien, R.; Kopp-Schneider, A.; Blettner, M. Concordance analysis: Part 16 of a series on evaluation of scientific publications. *Dtsch. Ärztebl. Int.* **2011**, *108*, 515–521. [CrossRef] [PubMed]

27. Neuendorf, K.A. *The Content Analysis Guidebook*, 2nd ed; SAGE: Los Angeles, CA, USA, London, UK; New Delhi, India; Singapore; Washington, DC, USA; Melbourne, Australia; 2017.

28. Penglei, L.; Zhang, X.; Wang, W.; Zheng, H. Estimating aboveground and organ biomass of plant canopies across the entire season of rice growth with terrestrial laser scanning. *Int. J. Appl. Earth Obs. Geoinf.* **2020**, *91*, 102132. [CrossRef]

29. Jin, X.; Xu, X. Rmote sensing of leaf water content for winter wheat using grey relational analysis (GRA), stepwise regression method (SRM) and partial least squares (PLS). In Proceedings of the 2012 First International Conference on Agro-Geoinformatics (Agro-Geoinformatics), Shanghai, China, 2–4 August 2012; pp. 1–5.

30. Mountrakis, G.; Im, J.; Ogole, C. Support vector machines in remote sensing: A review. *ISPRS J. Photogramm. Remote Sens.* **2011**, *66*, 247–259. [CrossRef]

31. Sheykhmousa, M.; Mahdianpari, M.; Ghanbari, H.; Mohammadimanesh, F.; Ghamisi, P.; Homayouni, S. Support Vector Machine Versus Random Forest for Remote Sensing Image Classification: A Meta-Analysis and Systematic Review. *IEEE J. Sel. Top. Appl. Earth Obs. Remote Sens.* **2020**, *13*, 6308–6325. [CrossRef]

32. Chirici, G.; Mura, M.; McInerney, D.; Py, N.; Tomppo, E.O.; Waser, L.T.; Travaglini, D.; McRoberts, R.E. A meta-analysis and review of the literature on the k-Nearest Neighbors technique for forestry applications that use remotely sensed data. *Remote Sens. Environ.* **2016**, *176*, 282–294. [CrossRef]

33. Shahabi, H.; Shirzadi, A.; Ghaderi, K.; Omidvar, E.; Al-Ansari, N.; Clague, J.J.; Geertsema, M.; Khosravi, K.; Amini, A.; Bahrami, S.; et al. Flood Detection and Susceptibility Mapping Using Sentinel-1 Remote Sensing Data and a Machine Learning Approach: Hybrid Intelligence of Bagging Ensemble Based on K-Nearest Neighbor Classifier. *Remote Sens.* **2020**, *12*, 266. [CrossRef]

34. Chen, Q.; Yang, X.; Ouyang, Z.; Zhao, N.; Jiang, Q.; Ye, T.; Qi, J.; Yue, W. Estimation of anthropogenic heat emissions in China using Cubist with points-of-interest and multisource remote sensing data. *Environ. Pollut.* **2020**, *266*, 115183. [CrossRef]

35. Yu, D.; Zha, Y.; Sun, Z.; Li, J.; Jin, X.; Zhu, W.; Bian, J.; Ma, L.; Zeng, Y.; Su, Z. Deep convolutional neural networks for estimating maize above-ground biomass using multi-source UAV images: A comparison with traditional machine learning algorithms. *Precis. Agric.* **2022**, *24*, 92–113. [CrossRef]

36. De Souza, R.; Peña-Fleitas, M.T.; Thompson, R.B.; Gallardo, M.; Padilla, F.M. Assessing Performance of Vegetation Indices to Estimate Nitrogen Nutrition Index in Pepper. *Remote Sens.* **2020**, *12*, 763. [CrossRef]

37. Wood, F.A.; Barker, W.G. Stem Pigmentation in Lowbush Blueberry. *Plant Physiol.* **1963**, *38*, 191–193. [CrossRef] [PubMed]

38. Duy, J.C. A Survey of the Quantitative Intraspecific Variation of Anthocyanins, Phenolics and Antioxidant Capacity in Leaves and Fruit of *Vaccinium angustifolium* Aiton Clones in Nova Scotia. Master's Thesis, Acadia University, Wolfville, NS, Canada, 1999.

39. Yue, J.; Feng, H.; Jin, X.; Yuan, H.; Li, Z.; Zhou, C.; Yang, G.; Tian, Q. A Comparison of Crop Parameters Estimation Using Images from UAV-Mounted Snapshot Hyperspectral Sensor and High-Definition Digital Camera. *Remote Sens.* **2018**, *10*, 1138. [CrossRef]

40. Viña, A.; Gitelson, A.A.; Rundquist, D.C.; Keydan, G.; Leavitt, B.; Schepers, J. Monitoring Maize (*Zea mays* L.) Phenology with Remote Sensing. *Agron. J.* **2004**, *96*, 1139–1147. [CrossRef]

41. Percival, D.; Anku, K.; Langdon, J. Phenotype, phenology, and disease pressure assessments in wild blueberry fields through the use of remote sensing technologies. *Acta Hortic.* **2023**, *1381*, 123–130. [CrossRef]